

Magnetization plateau and quantum phase transitions in a spin-orbital model

Zu-Jian Ying^{1,2,3,a}, Angela Foerster², Xi-Wen Guan⁴, Bin Chen¹, and Itzhak Roditi³

¹ Department of Physics, Hangzhou Teachers College, Hangzhou 310012, P.R. China

² Instituto de Física da UFRGS, Av. Bento Gonçalves 9500, Porto Alegre 91501-970, Brazil

³ Centro Brasileiro de Pesquisas Físicas, Rua Dr. Xavier Sigaud 150, 22290-180 Rio de Janeiro, RJ, Brazil

⁴ Department of Theoretical Physics, Research School of Physical Sciences and Engineering, and Centre for Mathematics and its Applications, Mathematical Sciences Institute, Australian National University, Canberra ACT 0200, Australia

Received 28 October 2003 / Received in final form 8 January 2004

Published online 8 June 2004 – © EDP Sciences, Società Italiana di Fisica, Springer-Verlag 2004

Abstract. A spin-orbital chain with different Landé g factors and one-ion anisotropy is studied in the context of the thermodynamical Bethe ansatz. It is found that there exists a magnetization plateau resulting from the different Landé g factors. Detailed phase diagram in the presence of an external magnetic field is presented both numerically and analytically. For some values of the anisotropy, the four-component system undergoes five consecutive quantum phase transitions when the magnetic field varies. We also study the magnetization in various cases, especially its behaviors in the vicinity of the critical points. For the SU(4) spin-orbital model, explicit analytical expressions for the critical fields are derived, with excellent accuracy compared with numerics.

PACS. 75.30.Kz Magnetic phase boundaries (including magnetic transitions, metamagnetism, etc.) – 71.27.+a Strongly correlated electron systems; heavy fermions – 75.10.Jm Quantized spin models

1 Introduction

Orbital degeneracy in electron systems leads to rich and novel magnetic phenomena in many transitional metal oxides [1]. Among them are the orbital ordering and orbital density wave, which have been observed experimentally in a family of manganites [2]. A tractable model to describe 2-fold orbital degenerate system is the SU(4) model [3], which has attracted much attention [3–10]. In the one-dimensional case the model is exactly solvable by Bethe ansatz (BA) [5, 11]. An interesting question is to study the critical behavior of such a system in an external magnetic field, especially when different Landé g factors for spin and orbital sectors are involved. One may expect that the difference of g factors will bring about new physics as a result of the competition of the spin and orbital degrees of freedom. In reference [9], the authors studied the magnetic properties of the SU(4) model via BA, without taking different g factors into account, whereas numerical calculation was performed in reference [10] for the model with different g factors for up to 200 lattice sites. However, a full picture about the critical fields is still lacking. Another motivation is to see whether or not any magnetization plateau (MP), an interesting magnetic phenomenon, occurs in such a spin-orbital model. As is well-known, antiferromagnetic chains with integer spin are

gapful [12], whereas for half-integer spin there also exists a gapful phase with a MP in the presence of a large planar anisotropy [13]. Also fractional MP have been observed and can be explained by Shastry-Sutherland lattice [14]. But an MP arising from different Landé g factors has not been addressed yet.

Deviation from the SU(4) symmetry can be caused by variation in the interaction parameters of neighbor sites [4, 6, 8, 15], while another possible deviation may result from the one-ion interaction. Since many compounds are magnetically anisotropic in which the orbital angular momentum (OAM) may be constrained in some direction due to crystalline field, the angle between spin and OAM determines the spin-orbital coupling (SOC) energy. This kind of one-ion SOC leads to magnetic anisotropy [16]. Under the influence of molecular field and an external field, the spin is parallel to the OAM. In such a case, $s_i^z \tau_i^z$ type of interaction describes well the SOC energy. Another possibility of such an interaction can be found when τ_i is pseudospin. In fact, some realizations of the SU(4) spin-orbital model were presented from tetrahis (dimethylamino) ethylene(TDAE)-C₆₀ [15] and semiconducting quantum dot array [17] involving two orbitals $l^z = 1, -1$, while the $l^z = 0$ orbital is excluded due to a higher crystal field energy in TDAE-C₆₀ or filled in the quantum dots due to lower energy in harmonic-oscillator potential. If the SOC is taken into account, we will have the anisotropy $s_i^z \tau_i^z$ by an effective relation $\mathbf{l} \cdot \mathbf{s} = 2\tau^z s^z$,

^a e-mail: ying@cbpf.br

since the $l^z = 0$ orbital is excluded and the transition caused by l^\pm in the SOC is prohibited. Here we shall introduce such an $SU(2) \otimes SU(2)$ SOC interaction into the $SU(4)$ model. A detailed investigation of the phase diagram is undertaken both numerically and analytically in the context of the thermodynamical Bethe ansatz (TBA). We find that the system exhibits an MP resulting from different g factors when the SOC is sufficiently strong. The critical behavior of the magnetization in the vicinities of the critical points is revealed. For certain values of Landé g factor, the model undergoes five consecutive quantum phase transitions when the external magnetic field varies. Further, the explicit analytic expressions for the critical fields for the $SU(4)$ model are derived, with excellent accuracy compared to numerical results.

2 The model and TBA

We shall consider an L-site chain with the Hamiltonian

$$\mathcal{H} = \mathcal{H}_0 + \mathcal{H}_z + \mathcal{M}, \quad \mathcal{H}_0 = \sum_{i=1} P_{i,i+1},$$

$$\mathcal{H}_z = \Delta_z \sum_i s_i^z \tau_i^z, \quad \mathcal{M} = -g_s H \sum_i s_i^z - g_t H \sum_i \tau_i^z, \quad (1)$$

where \mathbf{s} and $\boldsymbol{\tau}$ are spin-1/2 operators for spin and orbital sectors. The g_s denotes the Landé g factor in z -direction for spin sector and the orbital g factor g_t depends on the orbitals the system involves. For example, $g_t = 0$ in z -direction if only e_g orbitals involve and t_{2g} orbitals are already occupied [1], since the field energy is zero for the orbital $d_{x^2-y^2}$ while it is prohibited for the transition induced by the field from the orbital $d_{3z^2-r^2}$ to the occupied d_{xy} ; for $l^z = \pm 1$ orbitals [15,17] g_t is the real orbital g factor in z -direction multiplied by 2. We shall discuss generally and assume $g_s > g_t$ throughout the paper, the results for $g_s < g_t$ are similar when the spin and orbital sectors are exchanged. \mathcal{H}_0 is the $SU(4)$ model with $P_{i,j} = (2\mathbf{s}_i \cdot \mathbf{s}_j + 1/2)(2\boldsymbol{\tau}_i \cdot \boldsymbol{\tau}_j + 1/2)$ exchanging the four site states $|s_i^z \tau_i^z\rangle$: $\phi_1 = |\uparrow\downarrow\rangle$, $\phi_2 = |\downarrow\uparrow\rangle$, $\phi_3 = |\uparrow\uparrow\rangle$, $\phi_4 = |\downarrow\downarrow\rangle$. It should be noted that electrons have positive Δ_z whereas holes have negative Δ_z according to their SOC [18]. The symmetry is broken into $SU(2) \otimes SU(2)$ by \mathcal{H}_z and further into four $U(1)$'s by the external magnetic field H . The model can be solved exactly via BA approach. The BA equations are the same as the $SU(4)$ model [5,11] under the periodic boundary conditions, with the energy eigenvalues given by

$$E = -2\pi \sum_{i=1}^{M^{(1)}} a_1(\lambda_i) + \sum_{k=1}^4 E_k N_k, \quad (2)$$

where $a_n(\lambda) = 1/(2\pi) \ln(\lambda^2 + n^2/4)$, and $E_1 = -\Delta_z/4 - g_-H/2$, $E_2 = -\Delta_z/4 + g_-H/2$, $E_3 = \Delta_z/4 - g_+H/2$, $E_4 = \Delta_z/4 + g_+H/2$, with $g_\pm = g_s \pm g_t$. N_k is the total site number in state ϕ_k and $M^{(i)}$ ($i = 1, 2, 3$) is the rapidity number. For a certain choice of the basis order, which depends on whether or not

the component is energetically favorable, the energy can be rewritten as $E = \sum_{i=1}^{M^{(1)}} g^{(1)}(\lambda_i) + g^{(2)}M^{(2)} + g^{(3)}M^{(3)}$. Following references [19,20], one may obtain the ground state (GS) equations for the dressed energies $\epsilon^{(i)}$ ($i = 1, 2, 3$),

$$\epsilon^{(i)} = g^{(i)} - a_2 * \epsilon^{(i)-} + a_1 * (\epsilon^{(i-1)-} + \epsilon^{(i+1)-}), \quad (3)$$

where $\epsilon^{(0)} = \epsilon^{(4)} = 0$ and the symbol $*$ denotes the convolution. The GS is composed of Fermi seas filled by negative dressed energies $\epsilon^{(i)-}$. According to an energetics argument, we may divide the external field H into three regions: (I) $0 \leq H < H_{R1}$, (II) $H_{R1} < H < H_{R2}$, (III) $H_{R2} < H < \infty$ with $H_{R1} = |\Delta_z|/(2g_s)$, $H_{R2} = |\Delta_z|/(2g_t)$. For $\Delta_z > 0$, the corresponding basis order are: (I₊) $(\phi_1, \phi_2, \phi_3, \phi_4)^T$, (II₊) $(\phi_1, \phi_3, \phi_2, \phi_4)^T$, (III) $(\phi_3, \phi_1, \phi_2, \phi_4)^T$; for $\Delta_z < 0$: (I₋) $(\phi_3, \phi_4, \phi_1, \phi_2)^T$, (II₋) $(\phi_3, \phi_1, \phi_4, \phi_2)^T$, (III) the same as $\Delta_z > 0$. These five basis orders provide a full description of the phase diagram of the system.

3 Magnetization plateau

The competition between the anisotropy parameter Δ_z and the magnetic field H results in a novel quantum phase diagram. In the absence of the magnetic field, it is easy to find that the states ϕ_3 and ϕ_4 are gapful for $\Delta_z > \Delta_z^c = 4 \ln 2$. Whereas for $\Delta_z < -\Delta_z^c$, the components ϕ_1 and ϕ_2 are gapful. Therefore, the GS is in an $su(2)$ spin-orbital liquid state in strong anisotropy regime in the absence of the field. However, the presence of the magnetic field completely splits all four components energetically. The magnetization $M^z = g_s s^z + g_t \tau^z$ increases from zero. For large positive Δ_z , the field bring the component ϕ_3 closer to the GS, while the component ϕ_2 gradually gets out of the GS. Certainly, if the field reaches the first critical field where the component ϕ_3 has not yet involved in the GS, a quantum phase transition from the spin-orbital liquid phase to a ferromagnetic phase occurs. Thus a magnetization plateau opens with a constant magnetization $M^z = g_-/2$. Nevertheless, this plateau will end when the field is strong enough $H > H_{c2}^p$, the component ϕ_3 becomes involved in the GS. The critical field H_{c2}^p indicates a quantum phase transition from the ferromagnetic GS into a spin-orbital liquid phase. If the field continues to increase, the spin and orbital sectors become fully-polarized at the third critical point H_{c3}^p . From the TBA equations (3), we get the exact expressions for the critical fields

$$H_{c1}^p = \frac{4}{g_-}, \quad H_{c2}^p = \frac{\Delta_z/2 - 4}{g_t}, \quad H_{c3}^p = \frac{\Delta_z/2 + 4}{g_t}. \quad (4)$$

Notice that the plateau opens only if $\Delta_z > \Delta_z^p = 8g_s/g_-$ and $0 < g_t < g_s$. If the g factors are the same, the plateau disappears because the components ϕ_1 and ϕ_2 remain degenerate in the field. The critical behavior of the magnetization in the vicinities of the critical points may be

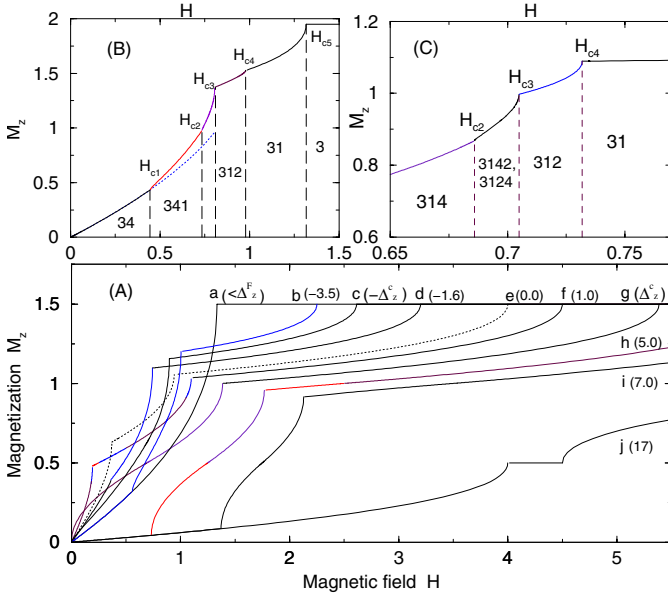


Fig. 1. (A) Typical magnetization behaviors for fixed values of Landé g factors $g_s = 2.0$ and $g_t = 1.0$. The numbers in brackets indicates values of the anisotropy parameter Δ_z . The dotted line e denotes the magnetization for the SU(4) model. Curve j exhibits a magnetization plateau. (B) Magnetization corresponding to five consecutive five H_c quantum phase transitions for $g_s = 2.0$, $g_t = 1.9$, and $\Delta_z = -3.0$. Here the variation of the state component numbers is $2 \rightarrow 3 \rightarrow 4 \rightarrow 3 \rightarrow 2 \rightarrow 1$. The number i labels the state ϕ_i , e.g., the state components in the phase 123 are $\phi_1 \phi_2 \phi_3$ in which ϕ_1 is energetically the most favorable whereas ϕ_3 is the least favorable. The phase variations between H_{c2} and H_{c3} are $3412 \rightarrow 3142 \rightarrow 3124$. The dotted line for comparison is an extension of the phase 34 by assuming the components unchanged. (C) Magnetization for consecutive five H_c phase transitions for $g_s = 2.0$ and $g_t = 1.0$, with $\Delta_z = -1.4$. $H_{c1} = 0.531$ (transition $3142 \rightarrow 214$) and $H_{c5} = 3.33$ ($31 \rightarrow 3$) are relatively far away. The variation of the component numbers in the phase transitions is $4 \rightarrow 3 \rightarrow 4 \rightarrow 3 \rightarrow 2 \rightarrow 1$.

summarized as follows

$$\langle M^z \rangle \cong \langle M^z \rangle_c + \eta k_M \delta H^{\frac{1}{2}}, \quad (5)$$

where $\langle M^z \rangle_c = g_{\mp}/2$ are, respectively, plateau and saturation magnetizations. δH is the small deviation from the critical points and $\eta = \pm 1$ depending on M^z is increasing or decreasing. $k_M = g_-^{3/2}/\pi$ near H_{c1}^p and $k_M = g_t^{3/2}/\pi$ near H_{c2}^p and H_{c3}^p . The coefficients g_- and g_t in (4) and (5) can be easily understood, since only ϕ_1 and ϕ_2 exist in the GS before H_{c1}^p is reached, the differences of their field energy and magnetization are $g_- H$ and g_- respectively. While for $H_{c2}^p < H < H_{c3}^p$, only ϕ_1 and ϕ_3 compete in the GS, since ϕ_2 already gets out before ϕ_3 enters the GS. ϕ_1 and ϕ_3 differ in field energy by $g_t H$ and in magnetization by g_t . In Figure 1A we plot the magnetization curves for different values of Δ_z under some fixed values of the g factors, the corresponding quantum phase transitions can be easily understood from the phase diagram presented in the next section. Among these curves is included a plateau case, other values of g_s and g_t give similar plateaux with the plateau magnetization located in $g_-/2$.

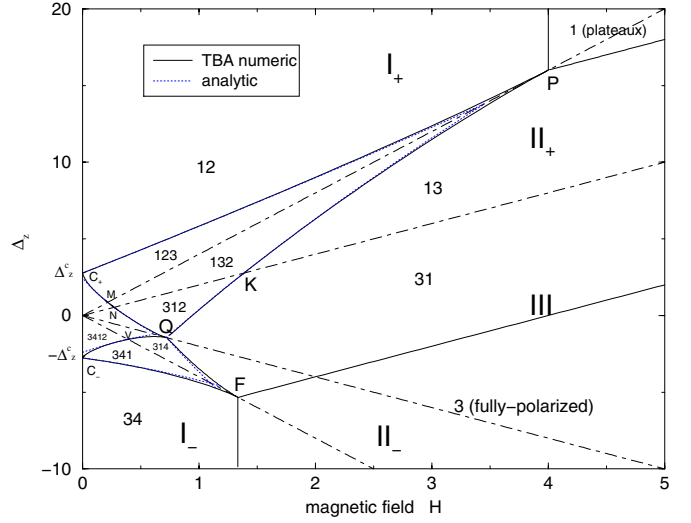


Fig. 2. Phase diagram for fixed values of Landé g factors $g_s = 2.0$ and $g_t = 1.0$. Inside C_+QC_- , the 4-state phases are 1234 (I₊), 1324 (II₊), 3124 (III), 3142 (II₋), and 3412 (I₋), with the energy $E_i < E_j < E_k < E_l$ corresponding to an order $ijkl$ in the respective sector (I_±, II_±, III). The discrepancy of the analytic curves from the numerical ones is not visible for most regions of C_+PQ and C_+MNQ (with typical differences within 1.0%, and 0.1%, respectively). There is less accuracy in regions I₋ and II₋ for the analytic results due to smaller Fermi boundaries. Magnetization plateaux and fully-polarized cases are exact.

4 The phase diagram: numerical and analytical

Here we present a detailed analysis of the GS phase diagram both numerically and analytically. In Figure 2, we plot the phase diagram with respect to Δ_z and H for fixed values of g_s and g_t ($g_s = 2.0$ and $g_t = 1.0$), phase diagrams for other values of g factors are presented in Figure 3B. For convenience, we refer to the GS with i components as i -state GS. Then for the phase transition between 3-state and 2-state GS, the critical fields follow from the Wiener-Hopf method [21], which is valid for large Fermi boundary (Fermi surface in one dimension). Explicitly, we have

$$\begin{aligned} H_c^{FC+} &\doteq (\Delta_z - \Delta_z^c) g_+^{-1} - \tau_1 g_-^2 g_+^{-3} (\Delta_z - \Delta_z^c)^2, \\ H_c^{QP} &\doteq \frac{\Delta_z^c + \frac{\Delta_z}{2}}{2g_s - g_t} + \tau_1 \frac{g_-^2 (\Delta_z - \Delta_z^K)^2}{(2g_s - g_t)^3}, \\ H_c^{QF} &\doteq \frac{\Delta_z^c - \frac{\Delta_z}{2}}{2g_s + g_t} + \tau_1 \frac{[g_t \Delta_z^c - (g_s + g_t) \Delta_z]^2}{(2g_s + g_t)^3}, \\ H_c^{FC-} &\doteq \pi^2 g_- g_+^{-2} \sqrt{1 - \tau_1 4g_-^2 g_+^2 (\Delta_z + \Delta_z^c) - 1}, \quad (6) \end{aligned}$$

where $\tau_1 = 1/(2\pi^2)$ and $\Delta_z^K = 2g_t H^K = g_t/g_- \Delta_z^c$ which corresponds to infinite Fermi boundary. Point Q

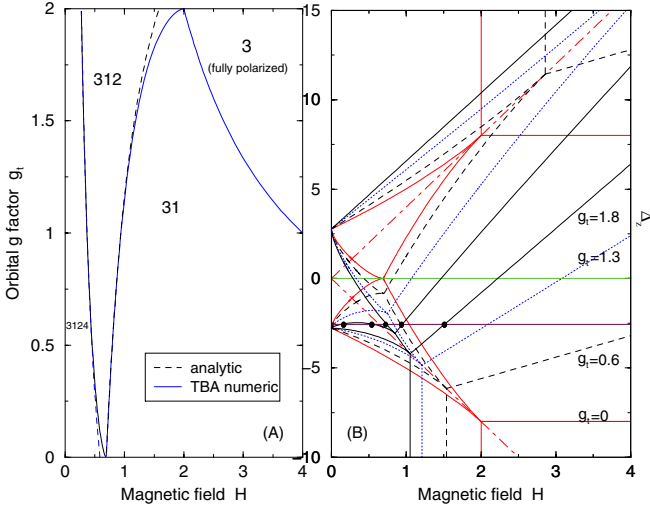


Fig. 3. (A) Comparison of the analytic and the numerical results for the three critical fields of the SU(4) model with respect to g_t for a fixed value $g_s = 2.0$. The numbers label the state components as in Figure 2, and H_{c3} (phase transition 31 → 3) is exact. (B) Phase diagrams for various g_t ($g_s = 2.0$). $\Delta_z = 0$ corresponds to the SU(4) model. The black dots mark consecutive five H_c phase transitions. Such a phenomenon exists for all $0 < g_t < g_s$, with H_{c1} - H_{c4} being closer for smaller g_t .

is determined by $\Delta_z^Q = -2g_t H^Q$, with $H^Q \doteq 2 \ln 2 / g_s + 4\pi^{-2} \ln^2 2 \times g_t^2 / g_s^3$. Near P or F the above analytic results deviate due to small Fermi boundary. But in this case, an analysis may be carried out in terms of expansion of small Fermi boundary. This leads us to $H_c^{PK}, H_c^{PC+} \cong \frac{\Delta_z}{2g_s} \pm (g_-/2)^{\frac{3}{2}} / (\pi g_s^{\frac{5}{2}}) (\Delta_z^P - \Delta_z)^{\frac{3}{2}}$. Similarly, near F, we have $H_c^{FQ}, H_c^{FC-} \cong -\frac{\Delta_z}{2g_s} \pm (g_+/2)^{\frac{3}{2}} / (\pi g_s^{\frac{5}{2}}) (\Delta_z - \Delta_z^F)^{\frac{3}{2}}$.

For $|\Delta_z| < \Delta_z^c$, the GS involves all the four components, the magnetic field first brings about a phase transition from a 4-component liquid to a 3-component liquid at the phase boundary C_+QC_- . Here one of the four components, which is energetically unfavorable, completely gets out of the GS, then the corresponding Fermi sea disappears. So the critical field only involves two Fermi boundaries B_1 and B_2 . At point C_+ , the component ϕ_2 is degenerate with the component ϕ_1 which is energetically the most favorable, the Fermi boundary B_1 lies at infinity. Increasing H along C_+MNQ drives ϕ_2 away from ϕ_1 , so ϕ_2 becomes energetically less favorable in the GS. Therefore the first Fermi sea shrinks, i.e., B_1 decreases from infinity. Beyond M point, both the increase of H and the decrease of Δ_z make ϕ_3 sink below the ϕ_2 which is rising, the energy difference between ϕ_3 and ϕ_1 begins to dominate over B_1 . As ϕ_3 is drawing near ϕ_1 , the first Fermi sea becomes broadened again with an increase of B_1 . After point N, ϕ_3 sinks beyond ϕ_1 to be the lowest state, ϕ_1 becomes less favorable in the GS. The first Fermi sea shrinks again, B_1 begins to decrease along NQ from the infinity at N. A similar analysis is applicable to B_2 , B_2 rises from zero at C_+ to infinity at M and decreases along MNQ to zero at

Q. In the respective sections of C_+MNQ the critical fields take the form

$$\begin{aligned} H_c^{C_+MNQ} &\doteq H_\infty^+ + H_{B_2}^{C_+MNQ} + wH_{B_1}^{C_+MNQ} \\ &\stackrel{MC_+}{=} H_\infty^+ + \tau_2 \Delta_{a,3}^2 / g_+ + w\tau_2 (g_- a_0 - g_t \Delta_{a,3})^2 / g_+^3 \\ &\stackrel{MN}{=} H_\infty^+ + \tau_2 [(g_- a_0 + g_s \Delta_{a,3})^2 + w(g_- a_0 - g_t \Delta_{a,3})^2] / g_+^3 \\ &\stackrel{NQ}{=} H_\infty^+ + \tau_2 (g_- a_0 + g_s \Delta_{a,3})^2 / g_+^3 + w\tau_2 \Delta_{a,3}^2 / g_+, \end{aligned} \quad (7)$$

where $H_\infty^+ = \Delta_{a,1} / g_+$, $\Delta_{a,m} = a_0 - \frac{m\Delta_z}{2}$, $a_0 = \frac{\sqrt{3}}{2}\pi - \frac{3}{2} \ln 3$, $\tau_2 = \frac{3}{16\pi^2}$, and $w = 2/3$. In each case, the first term comes from infinite B_1 and B_2 , the second term is correction from finite but large B_2 , and the third term is the leading correction from the larger B_1 . For C_+MN near point M the B_2 and B_1 terms need to be exchanged since B_2 becomes larger. Along NQ B_1 is always larger than B_2 . The location of $B_1 = B_2$ in C_+MN may be estimated by $H_{B_1} = H_{B_2}$, which gives $\Delta_z = 2a_0(2g_s - g_t) / (3g_s)$ for C_+M and $\Delta_z = \frac{2}{3}a_0$ for MN. This coincides well with numerics, e.g., for MC_+ and $g_s = 2.0$, $g_t = 1.0$, the analytic result is $\Delta_z = 1.073$ whereas the numerical one is 1.042.

Similarly, for C_-VQ , the term resulting from the infinite Fermi boundaries is $H_\infty^- = \Delta_{a,-1} / g_-$, the correction terms are $H_{B_2}^{VC-} = \tau_2 \Delta_{a,-3}^2 / g_-$, $H_{B_1}^{VC-} = H_{B_1}^{VQ} = \tau_2 [g_+ a_0 + g_t \Delta_{a,-3}]^2 / g_-^3$, and $H_{B_2}^{VQ} = \tau_2 [g_+ a_0 + g_s \Delta_{a,-3}]^2 / g_-^3$, respectively. These expressions are not valid for $g_s \sim g_t$ due to small Fermi boundaries.

When the system is fully-polarized, only ϕ_3 exists in the GS, while the other components are all gapful, with a gap $\Delta = \min\{E_i - 4 - E_3 \mid i = 1, 2, 4\}$. This gap is closed if $H < H_f$, with the fully-polarized critical point

$$H_f = \max\{(\Delta_z/2 + 4)g_t^{-1}, 4g_+^{-1}\}. \quad (8)$$

This expression is exact and valid for all Δ_z . When $\Delta_z \leq \Delta_z^F = -8g_s/g_+$, the strong negative anisotropy makes ϕ_1 and ϕ_2 too far away from ϕ_4 . Before the field brings them close enough to get involved in the GS, the component ϕ_4 has been all pumped out by the field from the GS at critical point $H_f = 4/g_+$. For all $\Delta_z \leq \Delta_z^F$, the magnetization is the same as shown by curve a in Figure 1A.

The analytic results are compared with the numerics in Figure 2, with very satisfactory accuracy.

5 Five consecutive H_c phase transitions

The competition of anisotropy Δ_z and the external field H also leads to an unusual magnetic phenomenon. For some fixed values of Δ_z , g_s and g_t , the system undergoes five consecutive quantum phase transitions when H varies, though the 4-component model usually has at most three consecutive phase transitions. A strong negative anisotropy Δ_z makes ϕ_4 energetically quite favorable. The field H expels ϕ_2 first from the 4-component GS. However, before H overwhelms the influence of Δ_z on ϕ_4 , further increase of H will make ϕ_2 closer to ϕ_4 and draw

it back into the GS. This process brings about the first two phase transitions. Then H plays a dominant role, it begins to bring out ϕ_4 , ϕ_2 and ϕ_1 from the GS one by one. This results in other three consecutive phase transitions. The variation of the state component numbers in the GS is: $4 \rightarrow 3 \rightarrow 4 \rightarrow 3 \rightarrow 2 \rightarrow 1$. This five H_c 's case exists for all $0 < g_t < g_s$ and becomes more visible when g_t is larger. One case is marked by black dots in Figure 3B for $g_s = 2.0$ and $g_t = 1.8$. Another possible case for five H_c transitions to occur is the GS composed of ϕ_3 and ϕ_4 . The field brings ϕ_1 into the GS first. As the difference of g_t and g_s is getting smaller, ϕ_2 has closer energy to ϕ_1 . Further increase of H brings ϕ_2 into the GS before ϕ_4 completely gets out. The component number changes in such a way: $2 \rightarrow 3 \rightarrow 4 \rightarrow 3 \rightarrow 2 \rightarrow 1$. This case occurs when the point Q is below C_- in Figure 2, approximately requiring $1 > g_t/g_s > 1 - 2 \ln 2g_t^3/(\pi^2 g_s^3)$. Four consecutive H_c transitions take place for $\Delta_z = -\Delta_z^c$. In Figures 1B and 1C, we plot the magnetization curves which display five consecutive H_c phase transitions. Such interesting phase transitions are more favorable to exist for holes, since holes have negative Δ_z as we mentioned below the Hamiltonian (1).

6 The SU(4) model

If we set the anisotropy parameter Δ_z to be zero, the model reduces to the SU(4) model with different Landé g factors in the spin and orbital sectors. In this special case, the above results for the critical fields give rise to

$$\begin{aligned} H_{c1}^{SU(4)} &\doteq a_0 g_+^{-1} + \tau_2 a_0^2 (2g_s - g_t)^2 g_+^{-3} + w \tau_2 a_0^2 g_+^{-1}, \\ H_{c2}^{SU(4)} &\doteq \Delta_z^c (2g_s - g_t)^{-1} + \tau_1 (g_t \Delta_z^c)^2 (2g_s - g_t)^{-3}, \\ H_{c3}^{SU(4)} &= 4g_t^{-1}. \end{aligned} \quad (9)$$

We compare the above analytic results with TBA numerical ones in Figure 3A, which shows an excellent accuracy for most values of g_t . Take $g_s = 2.0$ and $g_t = 1.0$ as an example, the analytic result for $H_{c1}^{SU(4)}$ and $H_{c2}^{SU(4)}$ are respectively 0.3697 and 0.9386 when TBA numerics gives 0.3695 and 0.9415 (also for comparison, 200 sites results [10]: 0.31, 0.93), the discrepancies are respectively only 0.05% and 0.3%. The analytic expression for $H_{c3}^{SU(4)}$ is exact. The magnetization of the SU(4) model is shown in Figure 1A, which also coincides with the numerical result for 200 sites [10].

7 Conclusions and summary

Based on the thermodynamical Bethe ansatz, we have studied non-pertubatively the quantum phase transitions of a spin-orbital chain, in the presence of an SU(2)⊗SU(2) same-site anisotropy Δ_z and different g factors for spin and orbital sectors. Various phase diagrams for different values of Δ_z and different g factors are systematically presented both numerically and analytically. Magnetization plateau invoked by the different g factors of the spin

and orbital is found for sufficiently large anisotropy Δ_z , the critical fields of the plateau as well as the plateau-existence conditions are obtained exactly and the critical behavior is analyzed. Interestingly for some values of Δ_z and the g factors, the four-component system undergoes five consecutive quantum phase transitions when the magnetic field varies. Especially, we get very accurate expressions for the critical fields the SU(4) model.

We thank Huan-Qiang Zhou, You-Quan Li and M.T. Batchelor for discussions and comments. ZJY thanks FAPERGS and FAPERJ for partial support. AF thanks FAPERGS and CNPq. XWG thanks the Australian Research Council for support. BC is supported by National Nature Science Foundation of China under Grant No. 10274070 and Zhejiang Natural Science Foundation RC02068. IR thanks PRONEX and CNPq.

References

1. Y. Tokura, N. Nagaosa, *Science* **288**, 462 (2000)
2. E. Saitoh, S. Okamoto, K.T. Takahashi, K. Tobe, K. Yamamoto, T. Kimura, S. Ishihara, S. Maekawa, Y. Tokura, *Nature* **410**, 180 (2001)
3. Y.Q. Li, M. Ma, D.N. Shi, F.C. Zhang, *Phys. Rev. Lett.* **81**, 3527 (1998)
4. S.K. Pati, R.R.P. Singh, D.I. Khomskii, *Phys. Rev. Lett.* **81**, 5406 (1998)
5. Y.Q. Li, M. Ma, D.N. Shi, F.C. Zhang, *Phys. Rev. B* **60**, 12781 (1999)
6. F. Mila, B. Frischmuth, A. Deppeler, M. Troyer, *Phys. Rev. Lett.* **82**, 3697 (1999)
7. B. Frischmuth, F. Mila, M. Troyer, *Phys. Rev. Lett.* **82**, 835 (1999)
8. P. Azaria, A.O. Gogolin, P. Lecheminant, A.A. Nersesyan, *Phys. Rev. Lett.* **83**, 624 (1999)
9. Y. Yamashita, N. Shibata, K. Ueda, *Phys. Rev. B* **61**, 4012 (2000)
10. S.J. Gu, Y.Q. Li, *Phys. Rev. B* **66**, 092404 (2002)
11. B. Sutherland, *Phys. Rev. B* **12**, 3795 (1975)
12. F.D.M. Haldane, *Phys. Lett. A* **93**, 464 (1983)
13. M. Oshikawa, M. Yamanaka, I. Affleck, *Phys. Rev. Lett.* **78**, 1984 (1997)
14. K. Kodama et al., *Science* **298**, 395 (2002); K. Onizuka et al., *J. Phys. Soc. Jpn* **69**, 1016 (2000); G. Misguich, Th. Jolicoeur, S.M. Girvin, *Phys. Rev. Lett.* **87**, 097203 (2001); B.S. Shastry, B. Sutherland, *Physica B* **108**, 1069 (1981)
15. D.P. Arovas, A. Auerbach, *Phys. Rev. B* **52**, 10114 (1995)
16. J.C. Slonczewski, *Phys. Rev.* **110**, 1341 (1958)
17. A.V. Onufriev, J.B. Marston, *Phys. Rev. B* **59**, 12573 (1998)
18. C.P. Slichter, *Principles of magnetic resonance*, 3rd edn. (Springer-Verlag, New York, 1990)
19. M. Takahashi, *Prog. Theor. Phys.* **46**, 401 (1971)
20. C.N. Yang, C.P. Yang, *J. Math. Phys.* **10**, 1115 (1969)
21. M.G. Krein, *Usp. Mat. Nauk* **13**, 3 (1958)